Jurnal
Teknologi

Full Paper

A STUDY ON THE INJECTION RATE CHARACTERISTICS OF THE SOLENOID COMMON-RAIL INJECTOR UNDER USING A HIGH-PRESSURE FUEL SYSTEM

Vo Tan Chau[a*], Tran Dang Long[b], Huynh Ba Vang[c], Nguyen Minh Hoang[a], Ngo Hoang Phuc[a], Nguyen Quoc Sy[a]

[a]Faculty of Automotive Engineering Technology, Industrial University of Ho Chi Minh City (IUH), 12 Nguyen Van Bao Street, Go Vap District, Ho Chi Minh City, Vietnam
[b]Faculty of Transportation Engineering, Ho Chi Minh City University of Technology (HCMUT)-268 Ly Thuong Kiet Street, District 10, Ho Chi Minh City, Vietnam
[c]Faculty of Transportation Mechanical Engineering, The University of Da Nang, University of Science and Technology, 50000, Vietnam

Article history
Received
31 August 2022
Received in revised form
25 January 2023
Accepted
30 January 2023
Published Online
19 April 2023

*Corresponding author
votanchau@iuh.edu.vn

Graphical abstract

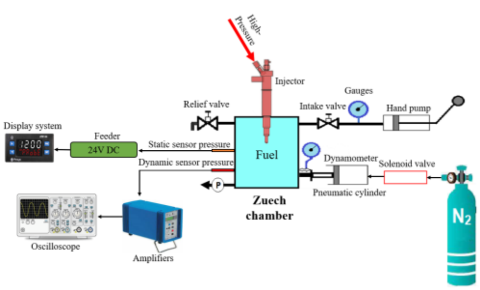

Abstract

The combustion of diesel engines is mainly controlled by fuel injection. Determining the fuel injection flow rate combined with the common-rail fuel injection system is a key solution to effectively improve engine performance and exhaust emissions. This work aims to investigate the influence of high injection pressures with a 6-holes-solenoid common rail injector on the injection rate characteristics in the range of 400 bar to 1600 bar, and a constant injector energizing time of 1.5 ms. The injection rate characteristics were carried out based on the pressure difference in the Zuech measuring chamber and synchronized data in real-time. The results showed that the increase of the mentioned injection pressures caused the decrease of hydraulic injection delay from 0.5 ms to 0.25 ms and expansion of the injector opening angle profile. In addition, the actual opening injection interval was prolonged as compared to the injector control signal. An increasing trend of fuel discharge coefficient was realized as higher injection pressure.

Keywords: Common-rail system, diesel engine, injection rate characteristics, zuech's method, solenoid injector

1.0 INTRODUCTION

Climate change has been viewed as a global environmental concern caused by humans. According to the Vietnam Directorate of Roads, transport vehicles are responsible for up to 70% of pollutant emissions in urban areas [1]. Propulsion systems, as well as vehicle-based diesel engines, seriously contribute to air pollution due to the large amount release of harmful emissions, especially NO_x and soot. A higher limitation of emission standards in the use of fuels derived from fossil has fostered stakeholders (researchers, automakers, government agencies, customers, etc) finding out effective solutions in using diesel engines as an essential part not only for transport means but also in energy supply systems. The top priority in improving the effect of fuel combustion is connected to the fuel injection process owing to its crucial influence on the sequence of atomization, spray evolution, air-fuel mixing, then engine performance along with emissions [2]. The combustible mixture formation is basically impacted by the movement of the intake airflow, the combustion chamber geometry, fuel, and the injection rate. Regarding these factors, the precise control of the injection rate to has played a key role in the process of mixing fuel with air because of the influence of momentum spray as the fuel exits the injector to boost the mixing process, the fuel injection rate profile is an important characteristic to consider in the desired trade-off soot and NO_x [3], the difference in injection rate shapes impacts to spray development such as spray penetration, liquid length, evaporation ratio...resulting in the change of air-fuel mixing process, then the intervention of emission formation [4], [5], [6].

Many researchers have investigated the efficiency of optimizing injection rate characteristics in terms of fuel consumption, emissions, and noise [7], [8], [9]. According to a study by A. L. Niculae *et al*. [10], the optimal rate of injection shape (triangular, trapezoidal, and boot) can simultaneously reduce NOx and soot by 11%, respectively 4% for maximum brake torque and by 22%, respectively 7% for maximum brake power using biodiesel B20, injection rate shape type Boot 2. Research by Z. Zhang *et al*. [11], V. Macian *et al*. [12], the shape of the injection rate profile (square, boot, ramp) as well as multiple injection strategies significantly induced the engine combustion and emission processes. D. A. Nehmer and R. D. Reitz [13], P. Karra, and S.C. Kong [14], who researched injection strategies, determined that one-time fuel injection with a high injection pressure of 200MPa produced the lowest soot emission. Regarding the emission standard of Tier 4, research results showed that the injection pressures in the range of 150MPa to 200MPa combined with a single injection at 5ATDC satisfied the soot concentration of this standard (0.4 g/kW-hr for NOx and 0.02 g/kW-hr for soot). In addition, the application of various injection conditions such as injection pressures, pilot injections, and EGR level (≥ 30%) can promote NOx emission to a level that is comparable to the Tier 4 standard. Keiki Tanabe *et al*. [2] gave the evaluation of the considerable impact on emissions and fuel consumption as varying injection pressures and injector-activated signal times. On this aspect, D. Han *et al*. [15] pointed out a higher injection pressure is shorter hydraulic injection delay and prolonger the actual injection duration. Several studies on injection rate under using the common rail system, for instance, F. Boudy and P. Seers [16], X. Seykens *et al*. [17], S. Yang and C. Lee [18], A. Boehman *et al*. [19] brang out the explanation by three effects: the first effect is the difference in injection pressure, due to the synchronization of the pressure wave with the time of injector lifting, the second effect is attributed to the friction coefficient during injection, and the other effect is related to the change of pressure wave amplitude. In addition, the influences of fuel properties on the amount of fuel injection and discharge coefficiency were carried out by D. Han *et al*. [15]. As known, the differences in biodiesel feedstock sources will result in their physical and chemical properties variances. The notable results of this research are the greater clarity on the effects of various biodiesel compositions such as Methyl laurate, Methyl oleate, and Ethyl oleate on injection characteristics as well as a significant impact of viscosity and bulk modulus in the change of injection rate characteristics. As a result, the study on fuel injection rate is critical in the design and optimization of operations to increase diesel engine efficiency and low emissions. In this work, the understanding of diesel injection rate behaviors for 6-holes-solenoid injector as adjusting injection pressures from common rail system was carried out to reach a relationship between injection pressures and relevant injection parameters such as the start of injection, actual injection duration, injection rate profile, injection quantity, fuel discharge coefficient. These achieved results may provide a good database related to accurately controlling the injection timing and quantity when using various injection pressures orienting the improvement of fuel economy and emission reduction.

2.0 METHODOLOGY

2.1 Injection rate-Zuech measurement method

In this study, fuel injection characteristics such as injection rate profile, hydraulic injection delay, effective injection duration, injection fuel quantity, and discharge coefficiency were gathered and analyzed by Zuech's flow measuring principle [20]. Figure 1 illustrates Zuech's injection rate measurement, in which, fuel is injected at a certain pressure into a compressed isovolumetric chamber of the same type of test fuel, with a value that corresponds to the pressure at the end of the compression stroke.

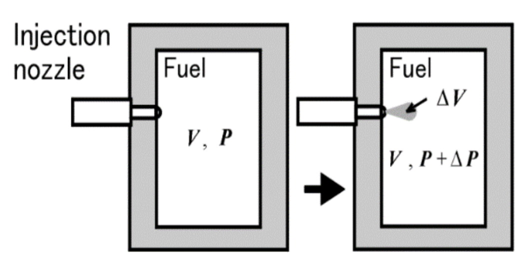

Figure 1 Injection rate measurement of Zuech [20]

The pressure in the measuring chamber rises in direct proportion to the amount of fuel injected at the time of injection. Hence, the injection rate is determined by sensing a change in pressure in the isovolumetric chamber. Specifically, when a volume of fuel (ΔV) is injected into a measuring chamber of volume (V), the pressure rise (ΔP) is determined by the following Equation [21]:

$$\Delta P = K.\frac{\Delta V}{V} \qquad (1)$$

where K is the modulus of elasticity (bulk modulus).

The injection rate ($\dot{m}_f$) will then be calculated according to Equation (2), which is formed from the measuring pressure rise in the constant volume chamber (1):

$$\dot{m}_f = \frac{d_m}{d_t} = \rho_f \frac{V}{K}\frac{\Delta P}{\Delta t} \qquad (2)$$

where ρ_f is the test fuel density.

The configuration of injection rate characteristics obtained from Equation (2) is displayed in Figure 2. This figure can be divided into 4 stages: injection delay phase, needle opening transition phase, quasi-steady phase (fully opening needle) and needle closing transition phase [22]. The hydraulic injection delay is calculated from when the control system sends a activate signal (SOE) to the injector until the time as injection starts (SOI), in which the initial injection rate curve changes from a negative value to zero and to a positive value [15], [22]y, [23]. The actual injection duration is counted from the start of injection (SOI) until the end of injection (EOI).

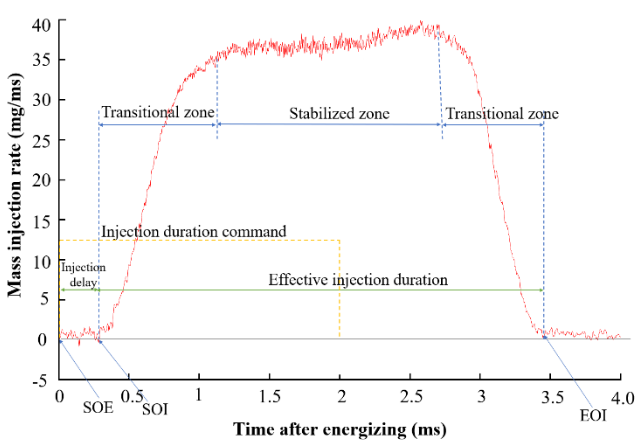

Figure 2 Definition of typical fuel injection rate (P = 800 bar, P_o = 45 bar, energizing time t = 1.5 ms)

The fuel discharge coefficient (C_d) in Equation (3) is defined as the ratio of the measured injection rate ($\dot{m}_f$) in Equation (2) to the theoretical injection rate determined by using the Bernoulli equation ($\dot{m}_{th}$) in Equation (4) [24]:

$$Cd = \frac{\dot{m}_f}{\dot{m}_{th}} \qquad (3)$$

$$\dot{m}_{th} = n.A..\sqrt{2\Delta P.\rho_f} \qquad (4)$$

where n is the number of injector nozzle holes, and A is the geometric area of the orifice.

The Reynolds coefficient characterizes the ratio between the inertial force and the frictional force in the injector and is determined by Equation (5):

$$Re = \frac{V.D}{\nu} \qquad (5)$$

where D is the diameter of the jet hole and ν is the fuel viscosity

V is the average speed. It is the velocity of the fuel flow in the injector calculated from Zuech's method and is shown in Equation (6).

$$V = \frac{\dot{m}_f}{n.A.\rho_f} \qquad (6)$$

2.2 Experimental setup and Test procedure

The injection rate measurement system for the common-rail diesel injector employed in this work can provide rail pressures up to 1600 bar and includes components as shown in Figures 3 and Figure 4. A solenoid injector G2 of 6 jet holes and 0.18 mm of orifice diameter was installed on top of a Zuech measurement chamber which had a volume of 43 cm^3 and fixed back pressure by a hydraulic fuel hand pump. The injector was coupled to a common rail injection system through a high-pressure common rail pump (HP3) which was driven by a 3-phase motor and inverter power high voltage. When the high-pressure pump was turned on, the test fuel will flow from the tank through the fuel filter, high-pressure pump, and compressed in an accumulator, injector. The Zuech measuring chamber was set up with a piezo transducer sensor (AVL GU12P) for detecting the pressure rise as an injection, and a static pressure sensor (Daho EDS 305) for motoring the back pressure. When fuel was injected, the signal from the piezo transducer sensor detected the pressure difference and was amplified by an amplifier (Kistler charge amplifier 5010B) before being sent to the data-acquisition device. The injector trigger signal, the fuel pressure in rail, and the fuel temperature were synchronized and indicated in real-time by a programmable microcontroller and Matlab programming.

Besides, a plunger with a diameter of 6.2 mm located in the Zuech chamber and a displacement of 3 mm is precisely controlled by a pneumatic cylinder assembled with a high-pressure Nitrogen (N_2) tank to calculate the fuel bulk modulus (K). The plunger's travel into the chamber reduces the chamber volume, which leads to an increase in pressure. Then, the fuel modulus of elasticity (K) was computed using Equation (1) and utilized as a correction factor when calculating the injection rate.

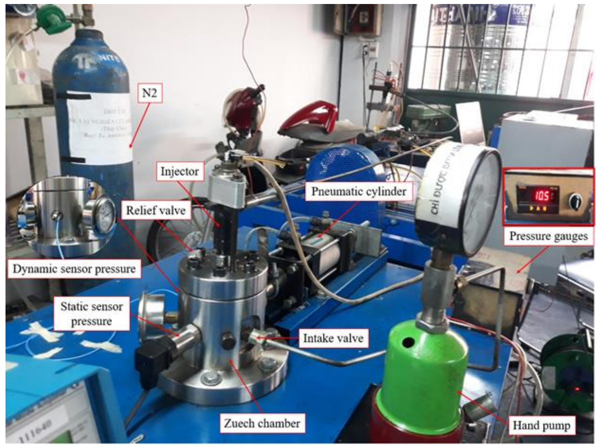

Figure 3 Photograph of the experimental set-up

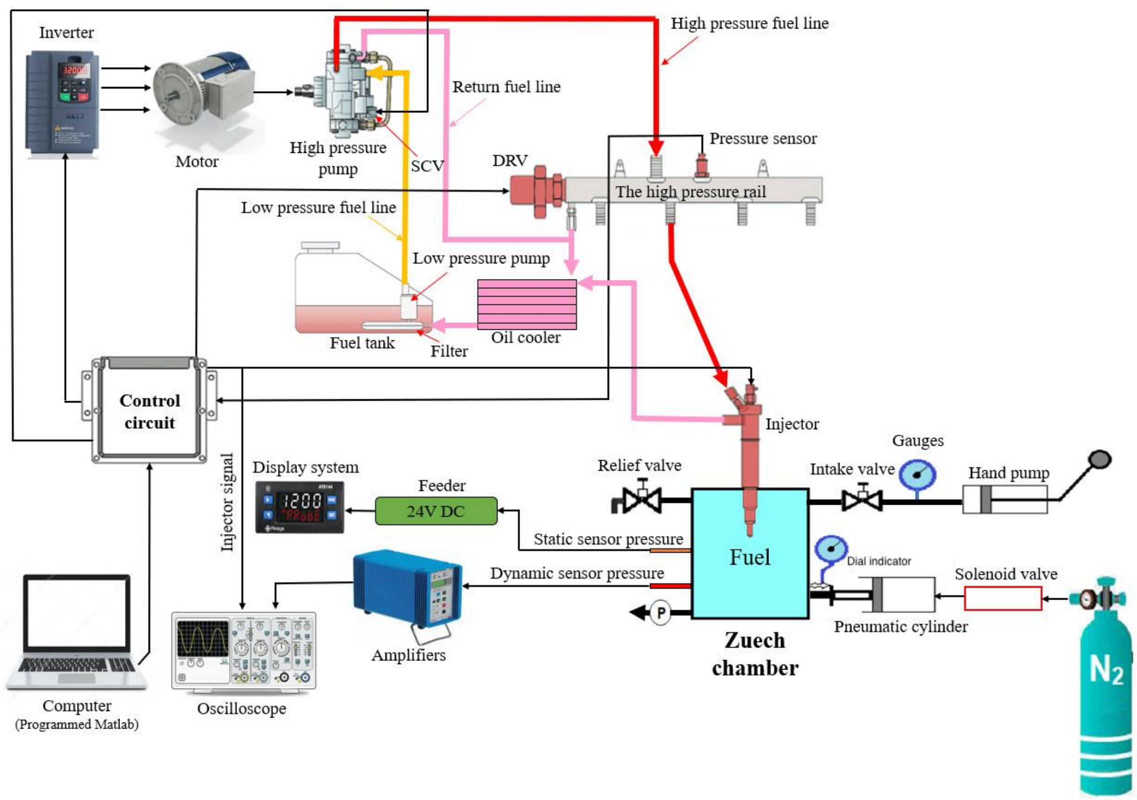

Figure 4 Schematic arrangement of experimental apparatus

2.3 Test Fuel and Test Conditions

The commercial diesel fuel in Vietnam was used in this study. Table 1 lists some chemical properties of diesel fuel.

Table 1 The Test Fuel Properties [26]

Parameter	Standard	Diesel
Molecular density at 15°C (Kg/m^3)	ASTM D4052	840
Kinematic Viscosity at 40°C (CST)	ASTM D445	3.07
Cetane	ASTM D4737	46

Table 2 Test Conditions

Parameters	Value
Fuel	Vietnam Commercial diesel
Injection pressure (P)	400 bar, 800 bar, 1200 bar, and 1600 bar
Energizing injection signal (ET)	1.5 ms
Back pressure in the Zuech chamber (P_o)	15 bar, 25 bar, 35 bar, 45 bar, 55 bar, 65 bar, and 75 bar
Injector	Solenoid G2, 6 holes, 0.18 mm of diameter
Number of repetitions/injection cycle	15 times

Table 2 illustrates the test conditions with a range of injection pressures from 400 bar to 1600 bar and a 1.5 ms of energizing injection control signal. The fuel elasticity is determined by varying the back pressure in the Zuech chamber from 15 bar to 75 bar to find the relation between fuel bulk modulus and back pressure which is seen as a simulating the late compression stroke. An average of 15 trials was used for each injection condition to calculate the injection rate.

3.0 RESULTS AND DISCUSSIONS

3.1 Fuel Bulk Modulus of Compressibility

The bulk modulus of fuel is a measure of its ability to withstand compression. It is defined as the ratio between the increased pressure in the chamber during compression to the relative decrease in the volume of the chamber [3]. Figure 5 shows the bulk modulus of diesel fuel at different back pressures in the measuring chamber which has the pressure value as a simulation of the real condition of the combustion chamber during injection process. Thereby, it can be seen that the bulk modulus linearly increases when the pressure in the measuring chamber increases. This is explained that, at high pressure, the compressibility of the fuel will decrease, because the compression of fuel molecules in the measuring chamber along with the increased pressure in the liquid prevents the reduction of fuel volume when the plunger enters the chamber causing the pressure rise in the chamber [27]. Therefore, bulk modulus will be inversely proportional to the compressive capacity, the tendency for bulk modulus to increase as the compressibility decreases. The difference in the fuel elasticity will directly affect the actual injection timing of the engine, then changing the combustion time and NOx emissions [28][29]. In addition, this difference will also affect the pressure wave of the fuel flowing in the high-pressure pipeline when changing the injection pressure, thereby affecting the injection rate profile and the actual amount of fuel injection [16].

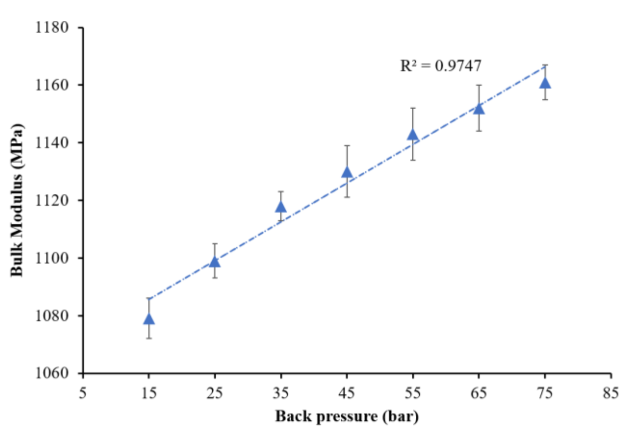

Figure 5 The modulus of elasticity under varying back pressures

3.2 The Relation between Injection Pressure and Injection Rate

The injection rate profile regulates the change in the injected amount of fuel during an injection cycle (from SOI to EOI), which also affects the distribution of fuel droplets and spray development in the combustion chamber. Figure 6 displays the effect of injection pressure on the injection rate curve of diesel fuel with the injector energizing time (ET) kept at 1.5 ms, the back pressure (P_o) of 45 bar and the injection pressure (P) varies from 400 bar to 1600 bar. The results show that the injection rate increases when increasing injection pressure owing to the higher flow capacity [30]. More specifically, at the injection pressure from 400 bar to 1200 bar, the average injection rate in the quasi-steady phase reached from 22.42 mg/ms to 49.35 mg/ms. The increasing percentage is about 45% to 50% after each injection pressure. Meanwhile, at an injection pressure of 1600 bar, the injection rate reached 56.43 mg/ms. This rate increased by about 15% compared to the previous injection. Furthermore, at the initial injector opening phase, the slope of the injection curve increases, indicating a large injector opening angle because the force acting on the injector's conical surface is now higher when increasing the pressure, resulting in an acceleration of the needle lifting process. It is noted that high injection pressure along with the optimal geometry of the nozzle hole helps to better blend the fuel, promotes the mixing of air and fuel, and contributes to reducing the amount of HC and black smoke in the exhaust. However, in order to reduce noise and NO_x emissions, the slope of the injection curve must be gradually increased in terms of the split injection strategy so that the fuel accumulation during the stage of the combustion delay is kept under a low level. Regarding the injection rate curve, with 1.5 ms of injector energizing time, it also illustrates a fully developed peak that is not too sharp to prevent the phenomenon of fuel not being finely atomized, leading to increased HC emissions, black smoke and increased fuel consumption during combustion [2].

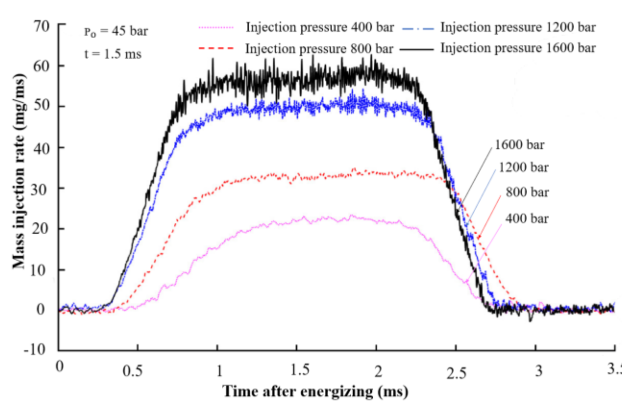

Figure 6 Effect of injection pressures on the injection rate under ET = 1.5 ms and P_o = 45 bar

3.3 Effects of Injection Pressure on Hydraulic Injection Delay

Figure 7 shows the hydraulic injection delay of diesel fuel at a back pressure of 45 bar, injector energizing time of 1.5 ms with injection pressure in the range from 400 bar to 1600 bar.

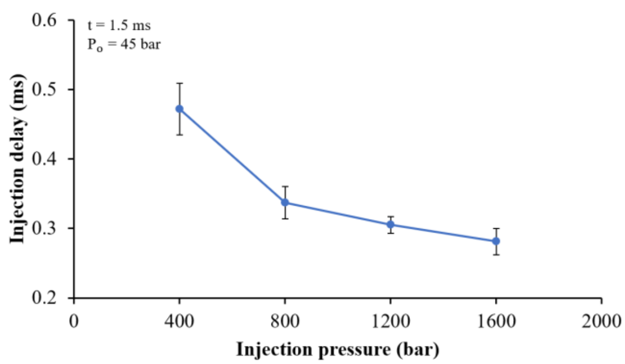

Figure 7 Hydraulic injection delay under varying injection pressures with ET = 1.5 ms and P_o = 45 bar

It is clearly observed that a higher injection pressure as mentioned above tends to decrease the injection delay from 0.5 ms to 0.25 ms, approximately. This is explained by the pressure difference formed between the control chamber when depressurized and the pressure exerted on the conical surface of the needle as the solenoid valve is activated. Moreover, with high injection pressures, the compressibility of fuel reduces so making higher thrust to lift the needle faster [15], [31]. In addition, fuel density and viscosity are closely related to fuel inertia and flow resistance, the higher injection pressure is a factor that speeds up the fuel flow out of the control chamber and nozzles create a shorter hydraulic injection delay [15], [32]. The change in hydraulic injection delay when varying injection pressure under these test conditions may impact the ignition delay phase leading to sequence effects of fuel consumption rate, noise, and emission (NO_x, HC) formation. This is consistent with the other studies [33], [34]. With the above factors, it needs to optimize the exact injection timing at the desired pressures to reduce emissions.

3.4 Effects of Injection Pressure on Actual Injection Duration

The actual injection duration is calculated from SOI until EOI as defined in Figure 2. Figure 8 shows the experimental results performed at conditions of 45 bar back pressure, 1.5 ms injector energizing signal, and injection pressures ranging from 400 bar to 1600 bar. According to this figure, effective injection duration is longer than the constant injector energizing time of 1.5 ms. As raising the injection pressure, the actual injection duration is prolonged from 0.8 ms to 1.0 ms. This is due to the residual fuel under the injector obstructing the needle closing process. This obstacle effect is also caused by the high injection pressure, and fuel viscosity combined with an increase in fuel elasticity.

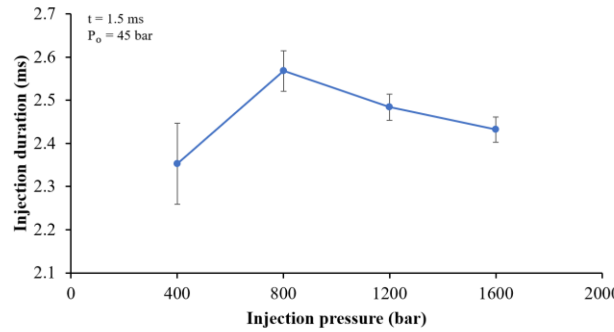

Figure 8 Actual injection duration under different injection pressures of solenoid injector with ET = 1.5 ms and P_o = 45 bar

This extension duration is not linear when increasing injection pressures. Specifically, when the injection pressure is gradually increased from 400 bar to 800 bar, the effective injection duration increases as compared to lower injection pressure. On contrary, for experiments conducted from 800 bar to 1600 bar, the effective injection length decreases. This reducing trend is similar to that demonstrated by Tomasz Knefel's study [31]. On the other hand, Prathan Srichhai *et al*. [30] attributed that as the injection pressure rises with a high elasticity coefficient, the fuel compression capacity in the control chamber of the injector decreases, leading to speed up the needle closing process. In addition, according to Plamondon and Seers [35], high fuel viscosity will limit the probability of leaking because the needle will close faster through the return oil hole as the power signal is off. With the aforementioned findings, the effects of longer injection length will take longer in the combustion process, resulting in higher fuel consumption, exhaust gas temperature, and HC emissions.

3.5 Effects of Injection Pressure on Injection Quantity

Figure 9 shows the fuel injection quantity at various pressures determined by integrating the injection rate profile. Generally, the amount of fuel injection increases with higher injection pressure because it reduces the fuel's compression capacity, enhancing the injection speed and the amount of fuel escaping from the injector. Detailly, injection pressures from 800 bar to 1600 bar provide fuel quantities of 70.18 mg, to 106.09 mg, in turn. It increases by around 15% to 30% after each injection pressure condition. Besides, one test condition concerned 400 bar of injection pressure, the injected mass reaches 36.51 mg. It is noted that an approximate increase of 92% under 800 bar of injection pressure compared to 400 bar of injection pressure. It is possible to demonstrate based on figure 6 that the injector opening angle is significantly smaller at low injection pressure, resulting in less fuel escaping from the injector. The injection quantity is affected by the properties of the fuel as well. In case fuel has a high viscosity, the pressure loss produced by friction in the pipeline must be considered in a reduction of the amount of fuel injected [30]. The measurement of fuel injection quantity has directly impacted the control of mixture equivalence ratio, which might timely intervene in emissions formation, improving power output and better fuel economy.

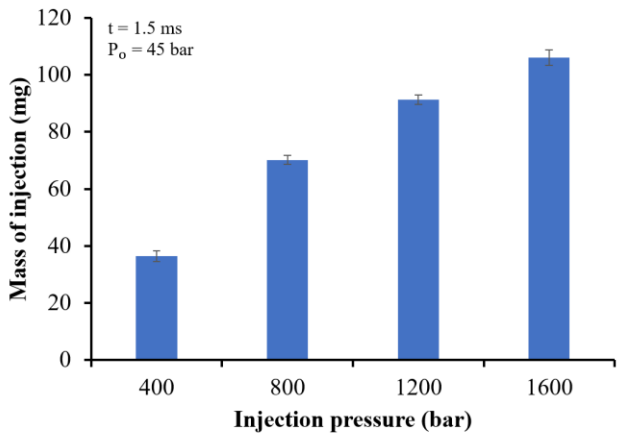

Figure 9 Injection quantity under different injection pressures of solenoid injector with ET = 1.5 ms and P_o = 45 bar

3.6 Effects of Injection Pressure on Fuel Discharge Coefficient

The fuel discharge coefficient is calculated using Equation (3) and plotted in Figure 10 at the conditions of injection pressure from 400 bar to 1600 bar, injector energizing time of 1.5 ms and back pressure of 45 bar.

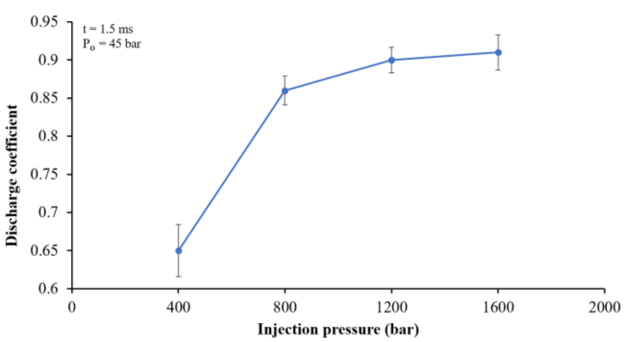

Figure 10 The impact of different injection pressures to discharge coefficient at ET = 1.5 ms and P_o = 45 bar

From the figure, an increasing trend is observed as higher injection pressure, which is consistent with studies by Dernotte *et al*. [32] and Padipan Tinprabath *et al*. [36], [37] for various biodiesels and single hole injectors. This is due to the fact that high injection pressure reduces the viscosity of the fuel, lowering pressure loss in the injectors [16], and resulting in improved fuel injection efficiency. Figure 11 displays the effect of the Reynold number on fuel injection efficiency for various injection pressures from 400 bar to 1600 bar. The results reveal that as the Reynolds number rises from 10,000 to 25,000, the fuel discharge coefficient rises, which is comparable to the trend in Figure 10 when injection pressure rises. This possibly demonstrates that the injection pressure and the Reynolds number have a relationship derived from the velocity of fuel flow out the orifices (Figure 6) based on the injection pressure rises.

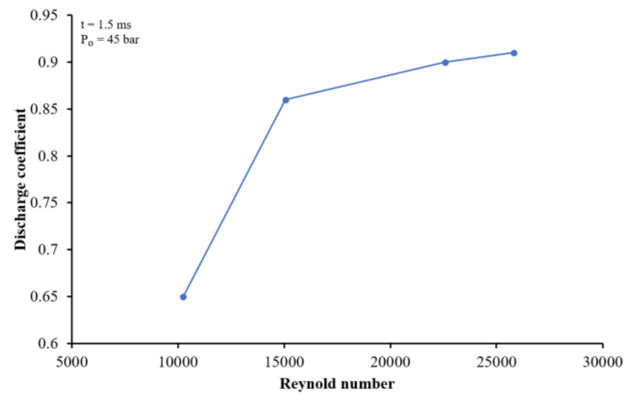

Figure 11 The impact of Reynold numbers to discharge coefficient at ET = 1.5 ms and P_o = 45 bar

4.0 CONCLUSION

The study of the injection characteristics for a 6-holes-solenoid diesel injector with different injection pressures on the high-pressure fuel 2nd generation common rail was conducted in a Zuech's chamber. The obtained results are concluded as follows:

The modulus of fuel elasticity proportionally increases with the higher injection pressures in the chamber. This impacts on speed up of needle lift of the injector resulting the adjustment of injection rate and the timing of injection opening and closing.

The hydraulic injection delay tends to decrease as the injection pressure increases. For different engine speeds and loads, the injection timing needs to be precisely distinguished to optimize the ignition delay phase to achieve low emissions.

Injection pressure is the core factor affecting the injection speed. With increased injection pressure, the injection mass increases due to increased flow capacity in the injector. Therefore, a consideration of injection quantity, injector energizing time, and injection timing must be applied when optimizing the engine operation to enhance engine performance, low emissions, and better fuel economy.

The actual injection duration is detected as longer than that of the given injector control signal. Furthermore, in this study, the different injection pressure ranges give the various tends of injector opening length relationship as classified into 2 groups: a group of 400 bar-800 bar is the low and the middle injection pressure that raises the effective injection duration as compared to levels of lower injection pressure; Group of over 800 bar is high injection pressure group gives the inverse trend of the previous mention.

The high injection pressure causes a lower pressure loss in the pipeline, resulting in an enhancement of the fuel discharge coefficient.

Conflicts of Interest

The author(s) declare(s) that there is no conflict of interest regarding the publication of this paper.

Acknowledgement

We acknowledge the support of time and facilities from Ho Chi Minh City University of Technology (HCMUT), VNU-HCM for this study.

References

[1] N. T. Anh and N. T. M. Tan. 2021. [Online]. Available: https://drvn.gov.vn/tin-tuc/tin-tuc-su-kien/van-de-o-nhiem-moi-truong-do-hoat-dong-giao-thong-do-thi-gay.html?site=20830. [Accessed 01 04 2022].

[2] K. Tanabe, S. Kohketsu and S. Nakayama, 2005. Effect of Fuel Injection Rate Control on Reduction of Emissions and Fuel Consumption in a Heavy Duty DI Diesel Engine. *SAE Technical Paper*.

[3] A. Takumura, S. Fukushima, Y. Omori and T. Kamimoto. 1989. Development of a New Measurement Tool for Fuel Injection Rate in Diesel Engines. *SAE Transactions*. 409-414.

[4] N. Intarat, L. Liu, D. Liu, X. Ma, and K. Nishida. 2020. An Analysis on the Effects of the Fuel Injection Rate Shape of the Diesel Spray Mixing Process Using a Numerical Simulation. *Applied Sciences*. 10(14): 4983. https://doi.org/10.3390/app10144983.

[5] L. Xu, X.S. Bai, M. Jia, Y. Qian, X. Qiao, X. Lu. 2018. Experimental and Modelling Study of Liquid Fuel Injection and Combustion in Diesel Engines with a Common Rail Injection System. *Applied Energy*. 230: 287-304. Doi: doi.org/10.1016/j.apenergy.2018.08.104

[6] F. Bai, Z. Zhang, Y. Du, F. Zhang and Z. Peng. 2017. Effects of Injection Rate Profile on Combustion Process and Emissions in Diesel Engine. *Journal of Combustion*. Doi: https://doi.org/10.1155/2017/9702625.

[7] P. L. Herzog, L. Bürgler, E. Winklhofer, P. Zelenka and W. Cartellieri. 1992. NOx Reduction Strategies for DI Diesel Engines. *SAE transactions*. 820-836.

[8] C. V. Beidl, D. W. Gill, W. Cartellieri and A. Rust. 1998. The Impact of Emissions and Fuel Economy Requirements on Fuel Injection System and Noise of HD Diesel Engines. *International Congress & Exposition*.

[9] V. H. Nguyen, A. Cavicchi, D. X. Nguyen, K. T. Nguyen, P. X. Pham and L. Postrioti. 2022. Hydraulic Characterization of a Second-generation Common Rail Injector Operating under Solo and Split Injection Strategies. *Flow Measurement and Instrumentation*. 85: 102170. Doi: 10.1016/j.flowmeasinst.2022.102170.

[10] A. L. Niculae, R. Chiriac, and A. Racovitza. 2022. Effects of Injection Rate Shape on Performance and Emissions of a Diesel Engine Fuelled by Diesel and Biodiesel B20. *Applied Sciences.* 12: 1333. Doi: 10.3390/app12031333.

[11] Z. Zhang, H. Liu, Z. Yue, Y. Wu, X Kong, Z. Zheng and M Yao. 2022. Effects of Multiple Injection Strategies on Heavy-duty Diesel Energy Distributions and Emissions under High Peak Combustion Pressures. *Frontiers in Energy Research*. Doi:10.3389/fenrg.2022.857077.

[12] V. Macian, R. Payri, S. Ruiz, M. Bardi abd A. H. Plazas. 2014. Experimental Study of the Relationship between Injection Rate Shape and Diesel Ignition using a Novel Piezo-Actuated Direct-acting Injector. *Applied Energy*. 118: 100-113. Doi: 10.1016/j.apenergy.2013.12.025.

[13] D. A. Nehmer and R. D. Reitz. 1994. Measurement of the Effect of Injection Rate and Split Injections on Diesel Engine Soot and NOx Emissions. *SAE transactions*. 1030-1041.

[14] P. Karra and S. C. Kong. 2009. Diesel Emission Characteristics using High Injection Pressure with Converging Nozzles in a Medium-duty Engine. *SAE International Journal of Fuels and Lubricants*. 1(1): 578-592.

[15] D. Han, Y. Duan, C. Wang, H. Lin and Z. Huang. 2014. Experimental Study on Injection Characteristics of Fatty Acid Esters on a Diesel Engine Common Rail System. *Fuel*. 123: 19-25. Doi: 10.1016/j.fuel.2014.01.048.

[16] F. Boudy and P. Seers. 2009. Impact of Physical Properties of Biodiesel on the Injection Process in a Common-rail Direct Injection System. *Energy Conversion and Management*. 50(12): 2905-2912. Doi: 10.1016/j.enconman.2009.07.005.

[17] X. L. J. Seykens, T. L. Somers and G. R. Baert. 2004. Modelling of Common Rail Fuel Injection System and Influence of Fluid Properties on Injection Process. *Proceedings of VAFSEP*. 6-9.

[18] S. Yang and C. Lee. 2018. Experimental Research on the Injection Rate of DME and Diesel Fuel in Common Rail Injection System by using Bosch and Zuech Methods. *Energies*. 11: 273. Doi.org/10.3390/en11020273.

[19] A. L. Boehman, D. Morris, J. Szybist and E. Esen. 2004. The Impact of the Bulk Modulus of Diesel Fuels on Fuel Injection Timing. *Energy & Fuels*. 18(6): 1877-1882. Doi: 10.1021/ef049880j.

[20] S. Ishikawa, Y. Ohmori, S. Fukushima, T. Suzuki, A. Takamura and T. Kamimoto. 2000. Measurement of Rate of Multiple-injection in CDI Diesel Engines. *SAE Technical Paper*. Doi: 10.4271/2000-01-1257.

[21] C. Arcoumanis, M. S. Baniasad and M. S. Banias. 1993. Analysis of Consecutive Fuel Injection Rate Signals Obtained by the Zeuch and Bosch Methods. *SAE Transactions*. 1371-1384.

[22] R. Munsin, Y. Laoonual, S. Jugjai, M. Matsuki and H. Kosaka. 2015. Effect of Glycerol Ethoxylate as an Ignition Improver on Injection and Combustion Characteristics of Hydrous Ethanol under CI Engine Condition. *Energy Conversion and Management*. 98: 282-289. Doi: 10.1016/j.enconman.2015.03.116.

[23] L. Postrioti, G. Buitoni, F. C. Pesce and C. Ciaravino. 2014. Zeuch Method-based Injection Rate Analysis of a Common-rail System Operated with Advanced Injection Strategies. *Fuel*. 128: 188-198. Doi: 10.1016/j.fuel.2014.03.006.

[24] R. Payri, A. García, V. Domenech, R. Durrett and A. H. Plazas. 2012. An Experimental Study of Gasoline Effects on Injection Rate, Momentum Flux and Spray Characteristics using a common Rail Diesel Injection System. *Fuel*. 97: 390-399. Doi: 10.1016/j.fuel.2011.11.065.

[25] B. T. B. Hue, N. K. Lien, D. V. D. Khoa, N. V. Dat, Q. Q. Huy, P. Q. Nhien, N. T. A. Hong, H. H. Tri and L. V. Thuc. 2012. Biodiesel Production from Rubber Seed Oil. *Can tho University Journal of Science*. 105-113.

[26] PETROLIMEX. 2011. DO oil. 22 12 2011. [Online]. Available: https://kv5.petrolimex.com.vn/nd/linhvuc-kd/nhien_lieu_diezen.html. [Accessed 15 04 2022].

[27] P. W. Bridgman. 1958. *The Physics of High Pressure*. London: George Bell & Sons. 116-149.

[28] J. B. Heywood. 1988. *Internal Combustion Engine Fundamentals.* New York: McGraw-Hill. 864.

[29] A. Monyem, J. H. Van Gerpen and M. Canakci. 2001. The Effect of Timing and Oxidation on Emissions from Biodiesel-fueled Engines. *Transactions of the ASAE*. 44(1): 35. Doi: 10.13031/2013.2301.

[30] P. Srichai, P. P. Ewphun, C. Charoenphonphanich, P. Karin, M. Tongroon and N. Chollacoop. 2018. Injection Characteristics of Palm Methyl Ester Blended with Diesel using Zuech's Chamber. *International Journal of Automotive Technology*. 19(3): 535-545.

[31] T. Knefel. 2011. The Evaluation of the Characteristic Injection Times of a Multiple Fuel Dose. *Journal of KONES*. 18: 205-213.

[32] J. Dernotte, C. Hespel, F. Foucher, S. Houillé and C. Mounaïm-Rousselle. 2012. Influence of Physical Fuel Properties on the Injection Rate in a Diesel injector. *Fuel*. 96: 153-160. Doi: 1016/j.fuel.2011.11.073.

[33] M. Wei, S. Li, J. Liu, G. Guo, Z. Sun and H. Xiao. 2017. Effects of Injection Timing on Combustion and Emissions in a Diesel Engine Fueled with 2, 5-dimethylfuran-diesel Blends. *Fuel*. 192: 208-217. Doi: 10.1016/j.fuel.2016.11.084.

[34] K. Santhosh and G. N. Kumar. 2021. Effect of Injection Time on Combustion, Performance and Emission Characteristics of Direct Injection CI Engine Fuelled with Equi-volume of 1-hexanol/diesel Blends. *Energy*. 214: 118984. Doi: 10.1016/j.energy.2020.118984.

[35] E. Plamondon and P. Seers. 2014. Development of a Simplified Dynamic Model for a Piezoelectric Injector using Multiple Injection Strategies with Biodiesel/diesel-fuel blends. *Applied Energy*. 131: 411-424. Doi: 10.1016/j.apenergy.2014.06.039.

[36] P. Tinprabath, C. Hespel, S. Chanchaona and F. Foucher. 2013. Influence of Biodiesel and Diesel Fuel Blends on the Injection Rate and Spray Injection in Non-vaporizing Conditions. *SAE Technical Paper*.

[37] P. Tinprabath, C. Hespel, S. Chanchaona and F. Foucher. 2015. Influence of Biodiesel and Diesel Fuel Blends on the Injection Rate under Cold Conditions. *Fuel*. 144: 80-89. Doi: 10.1016/j.fuel.2014.12.010.